# Semi-active Control of Structures Using Neuro-Predictive Algorithm for MR Dampers

**A. Karamodin[1], H.H. Kazemi[2] and M.R. Akbarzadeh-T[3]**

[1] *PhD student, Dept. of Civil Engineering , Ferdowsi University, Mashhad. Iran*
[2] *Professor, Dept. of Civil Engineering , Ferdowsi University, Mashhad. Iran*
[3] *Professor, Dept. of Electrical Engineering, Ferdowsi University of Mashhad, Iran*
*Email: akaramodin@yahoo.com, hkazemi@ferdowsi.um.ac.ir, akbarzadeh@ieee.org*

**ABSTRACT :**

A semi-active control method for a seismically excited nonlinear benchmark building equipped with a magnetorheological (MR) damper is presented and evaluated. A Linear Quadratic Gaussian (LQG) controller is designed to produce the optimal control force. The required voltage for the MR damper to produce the control force estimated by LQG controller is calculated by a neural network predictive control algorithm (NNPC). The LQG controller and the NNPC are linked to control the structure. The coupled LQG and NNPC system are then used to train a semi-active neuro-controller designated as SANC, which produces the necessary control voltage that actuates the MR damper. The effectiveness of the NNPC and SANC is illustrated and verified using simulated response of a 3-story full-scale, nonlinear, seismically excited, benchmark building excited by several historical earthquake records. The semi-active system using the NNPC algorithm is compared to the performance of passive as well as an active and a clipped optimal control (COC) system, which are based on the same nominal controller as is used in the NNPC algorithm. The results demonstrate that the SANC algorithm is quite effective in seismic response reduction for wide range of motions from moderate to severe seismic events, compared to the passive systems, and performs better than active and COC systems.

**KEYWORDS:** *structural Control; Predictive Control; Semi-active; Neural Network; Nonlinear, MR Damper*

## 1. INTRODUCTION

The magnetorheological (MR) damper is generating great interest among researchers in semi-active control of civil structures [1-6]. The MR damper is a smart semi-active control device that generates force in response to velocity and applied voltage. Consequently, semi-active control using MR dampers are powerful devices that enjoy the advantages of passive devices with the benefits of active control. Additionally, they are inherently stable, reliable, and relatively cost-effective; they require small activation power.

One challenge in the use of semi-active technology is in developing nonlinear control algorithms that are appropriate for implementation in full-scale structures. Numerous control algorithms have been adopted for semi-active systems. These algorithms are either conventional methods based on mathematical formulations [1-6] or intelligent methods based on neural networks or fuzzy logic [7–12].

Model Predictive Control (MPC) belongs to a class of algorithms that compute a sequence of manipulated variable adjustment in order to optimize the future behavior of a plant. A state model is used to predict the open-loop future behavior of the system over a finite time horizon from present states. The predicted behavior is then used to find a finite sequence of control actions which minimize a particular performance index within pre-specified constraints. It displays its main strength in its computational expediency, real-time applications, intrinsic compensation for time delays, treatment of constraints, and potential for future extensions of the methodology. Recent applications of MPC to the control of civil engineering structures have been demonstrated in Mei et al. [13-14].

Interest in a new class of computational intelligence systems known as artificial neural networks (ANNs) has grown in the last few several years. This type of network has been found to be a powerful computational tool for organizing and correlating information in ways that have been proven to be useful for solving certain types of problems that are complex and poorly understood. The applications of ANNs to the area of structural control have grown rapidly through system identification, system inverse identification or controller replication [7-9].Chang and Zhou [15] manipulated recurrent neural networks to emulate the inverse dynamics of the MR damper to predict the required voltage for full-state feedback closed-loop system. This model used to control a three-storey building subjected to El Centro earthquake record. Similarly, Bani-Hani and Mashal [8] proposed neural network to simulate the inverse model of an MR damper in a 6-story base-isolated building subjected to earthquake forces. Karamodin et al, [16] also used the inverse NN model of an MR damper to control a 3 story benchmark building subjected to different earthquake records, and compared the results to active and clipped optimal control (COC) [4] systems.

In this paper, a neural network predictive control (NNPC) algorithm is used to command the MR damper. Neural network predictive control is based on model predictive control (MPC) scheme. The NNPC is used to calculate voltage signals to be input to the MR damper so that it can produces desirable optimal control forces that is estimated by LQG control algorithm. The coupled LQG and NNPC system are then used to train a semi-active neuro-controller designated as SANC, which produces the necessary control voltage that actuates the MR damper. The effectiveness of the NNPC and SANC is illustrated and verified using simulated response of a 3-story full-scale, nonlinear, benchmark building excited by several historical earthquake records.

## 2. THREE-STORY BENCHMARK BUILDING

The 3-story benchmark buildings used for this study were designed for the Los Angeles region as defined by Ohtori et al. [17]. The building is 36.58 by 54.87 m in plan, and 11.89 m in height. Two far-field and two near-field historical ground motion records are selected for study: El Centro 1940, Hachinohe 1968, and Northridge 1994, Kobe 1995 earthquakes respectively. Control actuators are located on each floor of the structure to provide forces to adjacent floors. Because the actuator capacity is limited to a maximum force of 1,000 kN, three actuators are employed at the first floor and two actuators at each of the second and the third floors to provide the required larger forces. Three sensors for acceleration measurements are used for feedback in the control system on the first, second, and third floors.

## 3. MDEL PREDICTIVE CONTROL(MPC) SCHEME

The MPC scheme is based on an explicit use of a prediction model of the system response to obtain control actions by minimizing an objective function. The optimization objectives include minimization of the difference between the predicted and desired response and the control effort subject to prescribed constraints such as limits on the magnitude of the control force. In the MPC scheme, first a reference response trajectory yr(k) is specified. The reference trajectory is the desired target trajectory of the structural response. This is followed by an appropriate

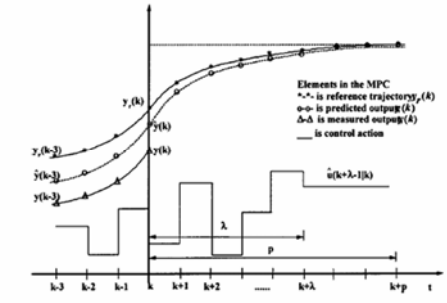


Figure 1. MPC scheme

prediction model which is then used to estimate the future building response y(k). The prediction is made over a pre-established extended time horizon using the current time as the prediction origin. For a discrete time model, this means predicting $\hat{y}(k+1), \hat{y}(k+2),.., \hat{y}(k+i)$ for i sample times in the future. This prediction is based on the past control inputs u(k), u(k-1),...,u(k-j) and on the sequence of future control efforts determined using the prediction model that are needed to satisfy a prescribed optimization objective. The control signals that were determined using the prediction model are then applied to the plant, and the actual plant system output y(k) is found. Finally, the actual measurement y(k) is compared to the model prediction $\hat{y}(k)$ and the prediction error [e (k)=y(k)- $\hat{y}(k)$ ] is utilized to update future predictions. Figure 1 describes schematically the basic MPC scheme.

## 4. PROPOSED CONTROL STRATEGY

### 4.1. *Neural Network Predictive Control (NNPC)*

Figure 2 illustrates the proposed control strategy. A Linear Quadratic Gaussian (LQG) controller is designed to produce the optimal control force. There is basically no restriction on the type of control algorithm that calculates a desirable control force $f_d$ based on response and/or excitation. The required voltage for the MR damper to produce the control force estimated by LQG controller is calculated by a neural network predictive control algorithm (NNPC) which is based on MPC scheme. NNPC consists of a neural network model of MR damper and an optimization algorithm (Figure 2). The neural network model is used to predict the open-loop future behavior of the MR damper over a finite time horizon from present states. The input to the neural network model is the velocity across the MR damper and voltage signal. The velocity which depends on the structural response is assumed to be constant over the horizon. The output of the neural network is the predicted damper forces which is then sent to the optimization algorithm, to find a finite sequence of control actions which minimize an objective function within pre-specified constraints. The objective function is the difference between the predicted and desired response and the control effort as shown below:

$$J = \sum_{j=1}^{N2} (y_r(t) - y_m(t+j))^2 + \rho \sum_{j=1}^{Nu} (u'(t+j-1) - u'(t+j-2))^2 \qquad (4.1)$$

where N2 and Nu, define the horizons over which the tracking error and the control increments are evaluated respectively. The desired control force is also assumed to be constant over the horizon. The output voltage of NNPC is input to the MR damper which then produces the force f, acting on the building.

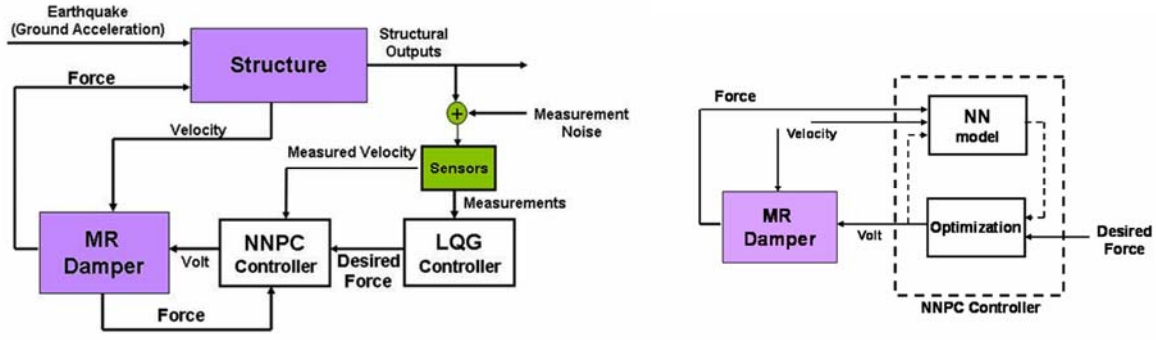


Figure 2: Control Strategy

### 4.2. *MR Model*

Adequate modeling of the control devices is essential for the accurate prediction of the behavior of the controlled system. The simple mechanical model shown bellow was developed and shown to accurately predict the

behavior of MR damper over a wide range of inputs [18-19]. This phenomenological model was developed based on a previous model used for an MR damper [21]. The equations governing the force f predicted by this model are as follows:

$$f = c_0 \dot{x} + \alpha z \tag{4.2}$$

$$\dot{z} = -\gamma \left| \dot{x} \right| z \left| z \right|^{n-1} - \beta \dot{x} \left| z \right|^{n} + A\dot{x} \tag{4.3}$$

where z is the evolutionary variable that accounts for the history dependence of the response. The model parameters depend on the voltage v to the current driver as follows:

$$\alpha = \alpha_a + \alpha_b u; \qquad c_0 = c_{0a} + c_{0b} u \tag{4.4a, b}$$

where u is given as the output of the first-order filter

$$\dot{u} = -\eta (u - v) \tag{4.5}$$

Eq. (4.5) is used to model the dynamics involved in reaching rheological equilibrium and in driving the electromagnet in the MR damper [20-21]. This MR damper model is used herein to model the behavior of the MR damper. The parameters of the MR damper were selected so that the device has a capacity of 1,000 kN, as follows: $\alpha_a$ = 1.0872e5 N/cm, $\alpha_b$ = 4.9616e5 N/(cm V), $c_{0a}$ = 4.40 N s/cm, $c_{0b}$ = 44.0. N s/(cm V), n=1, A=1.2, $\gamma$ =3 $cm^{-1}$, $\beta$ =3 $cm^{-1}$, and $\eta$ =50 $s^{-1}$.

### *4.3. Neural network Model of MR damper(NNMR)*

As discussed above, neural network predictive control (NNPC) proposed in this paper requires a neural network model of MR damper. The MR damper model discussed earlier in this paper estimates damper forces based on the inputs of the reactive velocity and the issued voltage as described by Equations (4.1)–(4.4). The damper velocity is the same as the relative velocity of the floors the damper is connected to. This neural network model is denoted as NNMR and is trained using input-output data generated analytically using the simulated MR model based on equations (4.1)–(4.4). NNMR calculates the damper forces based on the current and few previous histories of measured velocity, voltage signals and damper forces. Training the NNMR requires the compilation of input-output data. To completely identify the underlying MR system model, the data must contain information about the entire operating range of the system. Here, in this study, the velocity and voltage are generated randomly using band limited white Gaussian noise. The generated forces are results of the MR model described in equations (4.2)–(4.5). The sampling rate of the training data was 200 Hz for 30s period, which resulted in 6000 patterns for training, testing and validation (Figure 3). Next step is to select the network architecture. To do so, it is required to determine the numbers of inputs, outputs, hidden layers, and nodes in the hidden layers, and is usually done by trial and error. The most suitable input data for our case was found to be the current and the four previous histories for the velocity and voltage signal as well as five previous histories for the damper force. Also one hidden layer, with twenty nodes, was adopted as one of the best suitable topologies for the NNMR. The sigmoidal bipolar (tan-sigmoid; ranging from −1 to 1) activation function is used for the hidden layer and the linear function for the output layer which represents the voltage. 3000 patterns of the provided data were chosen for training which required 2000 training epochs to achieve a mean-square-error (MSE) of 1e−06.The training is carried out upon the generated data using the Levenberg–Marquardt algorithm [22], which is encoded in Neural Networks Toolbox in MATLAB [23] under ‘trainlm’ routine. Finally, testing and validation of the trained network is investigated using few sets of new data for a 30s period. Figure 4 shows the training testing and validation velocity, voltage and forces records used in constructing the NNMR model. It is clear that in general, the predicted forces are reasonably close to the target forces. The near perfect match in the training region indicates that the NNMR model is well trained.

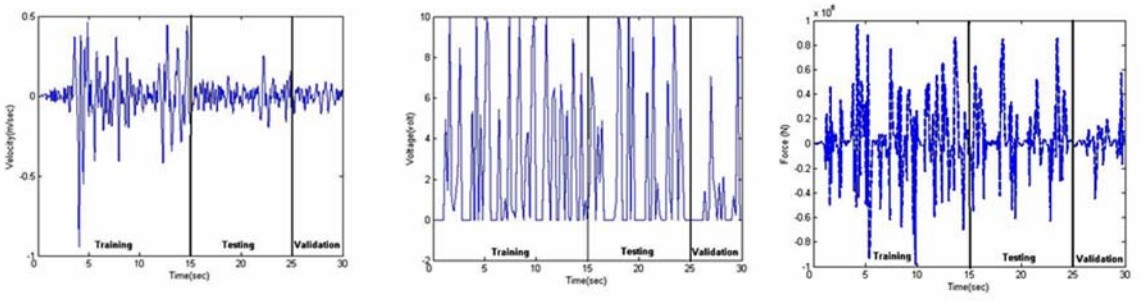


Figure 3: Training, testing and validation data for NNMR

4.4. ***Neural Network Controller***

As stated earlier the NNPC controller should minimize a performance index at each time step to find the required voltage for the MR damper to produce the desired force. This minimization is very time consuming and is not suitable for real time control.
Furthermore, The LQG and NNPC setup is used to train a single neural network that works as a stand-alone controller. This neural network is designated as SANC that estimates the control voltage for the semi-active device from the feedback sensors directly. Training the SANC controller is performed offline by generating the required training patterns when the structure is excited by 30 s of the El Centro earthquake record and controlled by the LQG and NNPC controller. A SIMULINK model was used to prepare the training data. The sampling rate is 200 Hz and the training patterns numbered 6000. The network architecture was designed to have 12 input neurons representing, the current and two previous histories of the accelerations of each story, in addition to one previous history of the dampers velocities which can be measured directly. One hidden layer having 20 hidden neurons was selected by trial and error. Finally, the output layer has three neurons, representing the control voltage for the semi-active devices. The sigmiodal bipolar (tan-sigmoid) activation function was used for the hidden layer and linear was used for the output layer (voltage). The provided 6000 patterns for training required 1000 training epochs to achieve a MSE of 1e−02.

## 5. CONTROL PERFORMANCE

The performance of the NNPC neural network is checked according to comparison of the force generated by MR damper to the ideal force estimated by LQG controller. Figure 4 shows the force generated by the MR damper at first floor of the building for Elcentro earthquake commanded by NNPC as compared to ideal force estimated by LQG controller. It can be seen that the damper forces follow the target optimal control forces closely. For evaluation of the proposed SANC controller the seismic effectiveness of MR dampers to reduce the response of the structure is considered. Both the drift ratio in the top story and acceleration time history at the top floor are compared in figure 5 with those of the uncontrolled structure under the different earthquakes. Although, the neuro-controller was trained by using El Centro earthquake, the roof acceleration and the relative displacement were considerably reduced after control action. Not only the peak responses, but also the overall amplitudes, were reduced in the responses.

Also the performance of the controllers are investigated based on the evaluation criteria specified (J1– J6) for the 3-story nonlinear benchmark building [17]. These criteria which are briefly presented in table1, are calculated as a ratio of the controlled and the uncontrolled responses. Ten earthquake records are used in the simulation, using the original four earthquake records with different intensities. These records are the Elcentro and Hachniohe earthquake records with 0.5, 1.0, and 1.5 intensity, and Northridge and Kobe earthquake records with 0.5 and 1.0 intensity. To make a comparison, an active control system and semi-active clipped optimal control (COC) system [4], together

with two passive systems, passive off (POFF-zero voltage) and passive on(PON-highest voltage), are simulated. Furthermore for evaluation the effectiveness of semictive control, two linear viscous passive control are also considered, These two passive control named as PV10 and PV15 are related to ten and fifteen percent critical damping in the first three modes of the structure respectively.

Table 2 presents the evaluation criteria as the ratio of the controlled response to the uncontrolled response for each earthquake record individually for active, COC, passive off, passive on, linear viscous damping and the proposed control systems. The average value of J1 and J4 for SANC, COC and active controller are 0.688, 0.728, 0.790 and 0.529, 0.854, 0.916 respectively. It can be concluded that SANC controller performs better than COC and active control to reduce the peak and norm drift. Also the average value of J2 and J5 for SANC, COC and active controller are 0.878, 0.889, 0.800 and 0.563, 0.795, 0.822 respectively which indicates that SANC has relatively equal performance to reduce the peak and norm of acceleration. The performance of NNPC is approximately equal to performance of active and COC in all criteria. Table 2 also shows that SANC is more effective in reduction of all criteria than passive off system. It can also be seen that the passive on system is the most effective in reduction of the peak and norm drift but, increases the acceleration of the structure. It can also be concluded that the performance of SANC in reducing the peak and norm of drift and acceleration is approximately equal to PV15, but performs better in reducing the peak and norm of base shear.

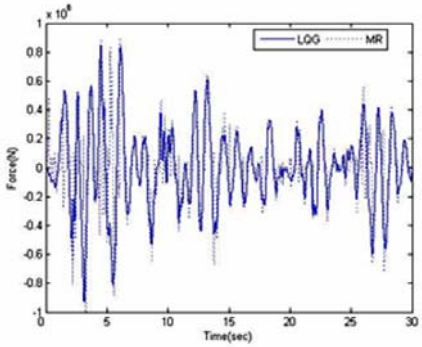


Figure 4: comparison of the force generated by MR damper to the ideal force (LQG)

## CONCLUSION

In this study, neural network predictive control (NNPC) have been used to predict the command voltage for MR damper to produce a target control force calculated from some optimal control algorithm ( LQG). Next, the LQG and NNPC coupled model operated in series manner to control the structure. The coupled model was then replaced by a single neural network (SANC) which produces the necessary voltage that generates the optimal control force in the MR damper.

A 3-story nonlinear benchmark building has been used for study. The results illustrate that it is possible to incorporate the NN models into the control strategy and hence operate the damper in an active mode. In general, the forces generated by the MR damper can follow those calculated from the optimal control algorithms. The effectiveness of controller for reducing the story drift and absolute acceleration of the structure have been checked and results show it performs very well for different earthquakes. The performance of the controller has also been compared to other control systems based on the evaluation criteria specified (J1– J6) for the benchmark building. The results show that SANC controller performs better than COC and active control to reduce the peak and norm drift ratio and has relatively equal performance to reduce the peak and norm of acceleration and base shear. The performance of NNPC is approximately equal to performance of active and COC in all criteria. Also SANC and NNPC perform better than passive off , passive on and linear viscous passive for all criteria unless the peak and norm drift which, passive on performs better than others.

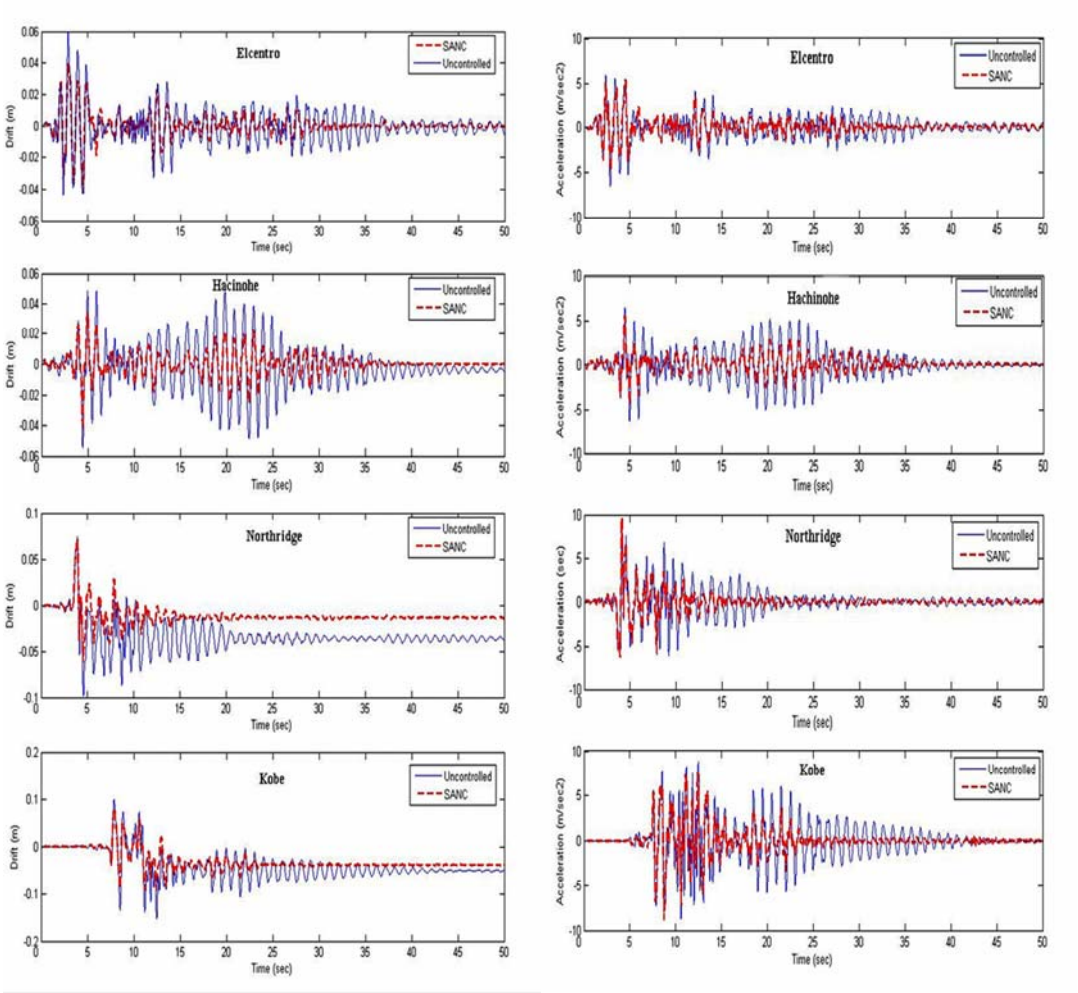


Figure 5. Comparison of the 3rd _floor story drift and acceleration of the structure for uncontrolled and SANC

Table 1. Performance criteria for seismically excited nonlinear building

| | | |
|---|---|---|
| **Interstory Drift Ratio** | **Level Acceleration** | **Base Shear** |
| $J_1 = \max_{\substack{\text{Ecentro}\\ \text{Hachinohe}\\ \text{Northridge}\\ \text{Kobe}}} \left\{ \frac{\max_{t,i} \frac{\lvert d_i(t) \rvert}{h_i}}{\delta^{max}} \right\}$ | $J_2 = \max_{\substack{\text{Ecentro}\\ \text{Hachinohe}\\ \text{Northridge}\\ \text{Kobe}}} \left\{ \frac{\max_{t,i} \lvert \ddot{x}_{ai}(t) \rvert}{\ddot{x}_{ai}{}^{max}} \right\}$ | $J_3 = \max_{\substack{\text{Ecentro}\\ \text{Hachinohe}\\ \text{Northridge}\\ \text{Kobe}}} \left\{ \frac{\max_{i} \left\lvert \sum_i m_i \ddot{x}_{ai}(t) \right\rvert}{F_b{}^{max}} \right\}$ |
| **Normed Interstory Drift** | **Normed Level Acceleration** | **Normed Base Shear** |
| $J_4 = \max_{\substack{\text{Ecentro}\\ \text{Hachinohe}\\ \text{Northridge}\\ \text{Kobe}}} \left\{ \frac{\max_{t,i} \frac{\lVert d_i(t) \rVert}{h_i}}{\delta^{max}} \right\}$ | $J_5 = \max_{\substack{\text{Ecentro}\\ \text{Hachinohe}\\ \text{Northridge}\\ \text{Kobe}}} \left\{ \frac{\max_{t,i} \lVert \ddot{x}_{ai}(t) \rVert}{\ddot{x}_{ai}{}^{max}} \right\}$ | $J_6 = \max_{\substack{\text{Ecentro}\\ \text{Hachinohe}\\ \text{Northridge}\\ \text{Kobe}}} \left\{ \frac{\max_{i} \left\lVert \sum_i m_i \ddot{x}_{ai}(t) \right\rVert}{\lVert F_b{}^{max} \rVert} \right\}$ |

Table 2: Performance criteria for passive, active, COC, NNPC and SANC algorithms

| | Controller | Elcentro 0.5 | Elcentro 1.0 | Elcentro 1.5 | Hachino 0.5 | Hachino 1.0 | Hachino 1.5 | Nortdridge0.5 | Nortdridge1.0 | Kobe 0.5 | Kobe 1.0 | Average |
|---|---|---|---|---|---|---|---|---|---|---|---|---|
| J1 | SANC | 0.467 | 0.662 | 0.876 | 0.406 | 0.666 | 0.695 | 0.561 | 0.891 | 0.988 | 0.664 | 0.688 |
| | NNPC | 0.562 | 0.763 | 0.848 | 0.681 | 0.800 | 0.816 | 0.675 | 0.949 | 0.839 | 0.651 | 0.758 |
| | Active | 0.544 | 0.753 | 0.873 | 0.637 | 0.768 | 0.794 | 0.826 | 1.035 | 0.819 | 0.854 | 0.790 |
| | COC | 0.457 | 0.704 | 0.883 | 0.541 | 0.697 | 0.706 | 0.714 | 0.950 | 0.881 | 0.752 | 0.728 |
| | POFF | 0.938 | 0.964 | 0.963 | 0.782 | 0.977 | 0.984 | 0.995 | 0.988 | 1.016 | 0.988 | 0.959 |
| | PON | 0.271 | 0.476 | 0.717 | 0.155 | 0.212 | 0.358 | 0.392 | 0.761 | 0.724 | 0.715 | 0.478 |
| | PV10 | 0.511 | 0.681 | 0.850 | 0.612 | 0.608 | 0.617 | 0.864 | 0.857 | 0.923 | 0.738 | 0.726 |
| | PV15 | 0.471 | 0.628 | 0.757 | 0.505 | 0.501 | 0.505 | 0.784 | 0.899 | 0.737 | 0.713 | 0.650 |
| J2 | SANC | 0.724 | 0.785 | 0.957 | 0.608 | 0.850 | 1.071 | 0.983 | 1.022 | 0.896 | 0.884 | 0.878 |
| | NNPC | 0.647 | 0.806 | 1.079 | 0.785 | 0.929 | 0.939 | 0.914 | 1.139 | 0.826 | 0.691 | 0.876 |
| | Active | 0.598 | 0.781 | 0.939 | 0.658 | 0.798 | 0.844 | 0.851 | 0.869 | 0.829 | 0.833 | 0.800 |
| | COC | 0.820 | 0.829 | 0.938 | 0.812 | 0.909 | 0.957 | 0.862 | 0.890 | 0.871 | 1.002 | 0.889 |
| | POFF | 0.966 | 0.998 | 1.000 | 0.886 | 0.999 | 0.963 | 1.012 | 1.003 | 0.918 | 0.997 | 0.974 |
| | PON | 0.649 | 0.881 | 1.142 | 0.721 | 0.439 | 0.738 | 0.795 | 1.019 | 1.102 | 0.800 | 0.829 |
| | PV10 | 0.539 | 0.885 | 0.985 | 0.646 | 0.708 | 0.967 | 0.941 | 1.048 | 0.971 | 0.765 | 0.846 |
| | PV15 | 0.504 | 0.828 | 0.956 | 0.559 | 0.613 | 0.858 | 0.862 | 1.001 | 0.971 | 0.872 | 0.803 |
| J3 | SANC | 0.509 | 0.940 | 1.066 | 0.625 | 0.847 | 1.023 | 0.917 | 0.965 | 0.950 | 0.999 | 0.884 |
| | NNPC | 0.580 | 0.969 | 0.974 | 0.588 | 0.804 | 0.962 | 0.912 | 1.054 | 0.905 | 1.045 | 0.879 |
| | Active | 0.507 | 0.881 | 0.914 | 0.553 | 0.779 | 0.925 | 0.831 | 0.819 | 0.851 | 0.966 | 0.803 |
| | COC | 0.583 | 1.043 | 1.062 | 0.574 | 0.797 | 0.923 | 0.910 | 0.943 | 0.994 | 1.006 | 0.883 |
| | POFF | 0.976 | 0.991 | 1.010 | 0.807 | 1.001 | 0.983 | 0.999 | 0.989 | 0.955 | 1.009 | 0.972 |
| | PON | 0.614 | 0.868 | 1.083 | 0.522 | 0.609 | 0.834 | 0.716 | 1.014 | 1.098 | 1.091 | 0.845 |
| | PV10 | 0.601 | 0.927 | 1.164 | 0.907 | 1.000 | 1.205 | 0.902 | 1.184 | 1.329 | 1.387 | 1.061 |
| | PV15 | 0.588 | 0.908 | 1.147 | 0.805 | 0.888 | 1.087 | 0.755 | 1.198 | 1.348 | 1.715 | 1.044 |
| J4 | SANC | 0.388 | 0.514 | 0.431 | 0.161 | 0.234 | 0.495 | 0.165 | 0.895 | 1.238 | 0.771 | 0.529 |
| | NNPC | 0.583 | 0.644 | 0.648 | 0.421 | 0.489 | 0.786 | 0.450 | 0.515 | 0.641 | 0.400 | 0.558 |
| | Active | 0.799 | 0.851 | 0.708 | 0.590 | 0.655 | 1.199 | 1.088 | 1.237 | 0.829 | 1.202 | 0.916 |
| | COC | 0.656 | 0.776 | 0.693 | 0.352 | 0.471 | 0.956 | 0.710 | 1.199 | 1.149 | 1.576 | 0.854 |
| | POFF | 0.892 | 1.062 | 0.817 | 0.807 | 0.930 | 0.922 | 1.025 | 1.051 | 1.122 | 0.961 | 0.959 |
| | PON | 0.183 | 0.245 | 0.267 | 0.118 | 0.107 | 0.134 | 0.077 | 0.792 | 0.436 | 0.193 | 0.255 |
| | PV10 | 0.504 | 0.707 | 0.788 | 0.303 | 0.312 | 0.337 | 0.245 | 0.666 | 1.552 | 0.250 | 0.567 |
| | PV15 | 0.376 | 0.528 | 0.464 | 0.224 | 0.230 | 0.225 | 0.186 | 0.985 | 1.009 | 0.424 | 0.465 |
| J5 | SANC | 0.612 | 0.690 | 0.681 | 0.337 | 0.365 | 0.449 | 0.611 | 0.668 | 0.569 | 0.648 | 0.563 |
| | NNPC | 0.609 | 0.705 | 0.690 | 0.447 | 0.508 | 0.587 | 0.635 | 0.673 | 0.592 | 0.670 | 0.612 |
| | Active | 0.764 | 0.931 | 0.925 | 0.561 | 0.685 | 0.814 | 0.878 | 0.914 | 0.821 | 0.926 | 0.822 |
| | COC | 0.781 | 0.945 | 0.932 | 0.570 | 0.565 | 0.704 | 0.861 | 0.887 | 0.794 | 0.915 | 0.795 |
| | POFF | 0.902 | 0.906 | 0.912 | 0.816 | 0.949 | 0.961 | 0.930 | 0.927 | 0.896 | 0.944 | 0.914 |
| | PON | 2.875 | 1.687 | 1.233 | 2.210 | 1.255 | 1.022 | 2.357 | 1.623 | 1.912 | 1.518 | 1.769 |
| | PV10 | 0.599 | 0.852 | 0.919 | 0.361 | 0.373 | 0.478 | 0.653 | 0.865 | 0.829 | 0.892 | 0.682 |
| | PV15 | 0.474 | 0.674 | 0.776 | 0.283 | 0.293 | 0.380 | 0.574 | 0.798 | 0.734 | 0.860 | 0.585 |
| J6 | SANC | 0.617 | 0.691 | 0.677 | 0.340 | 0.374 | 0.461 | 0.690 | 0.712 | 0.582 | 0.696 | 0.584 |
| | NNPC | 0.595 | 0.697 | 0.672 | 0.447 | 0.512 | 0.594 | 0.696 | 0.694 | 0.581 | 0.689 | 0.618 |
| | Active | 0.741 | 0.911 | 0.892 | 0.557 | 0.682 | 0.813 | 0.953 | 0.937 | 0.780 | 0.910 | 0.818 |
| | COC | 0.754 | 0.931 | 0.912 | 0.460 | 0.578 | 0.723 | 0.963 | 0.949 | 0.792 | 0.937 | 0.800 |
| | POFF | 0.901 | 0.901 | 0.908 | 0.818 | 0.954 | 0.966 | 0.944 | 0.926 | 0.891 | 0.938 | 0.915 |
| | PON | 0.913 | 0.790 | 0.748 | 0.641 | 0.515 | 0.509 | 0.897 | 0.799 | 0.751 | 0.847 | 0.741 |
| | PV10 | 0.590 | 0.857 | 0.936 | 0.372 | 0.384 | 0.490 | 0.708 | 0.927 | 0.878 | 0.991 | 0.713 |
| | PV15 | 0.473 | 0.688 | 0.804 | 0.303 | 0.313 | 0.404 | 0.657 | 0.913 | 0.803 | 1.010 | 0.637 |

REFERENCES

[1] Casciati, F., Magonette, G., and Marazzi, F. (2006).Technology of semi-active devices and application in vibration mitigation. John-Wiley,.
[2] Sack, R. L., Kuo, C. C., Wu, H. C., Liu, L. and Patten, W. N. (1994).Seismic motion control via semi-active hydraulic actuators. *Proc., U.S. 5th Nat. Conf. on Earthquake Engrg.,* **Vol. 2**,.311– 320.
[3] Sack, R. L., and Patten, W. (1994).Semi-active hydraulic structural control. *Proc., Int. Workshop on Struct Control*, Los Angeles. 417–431.
[4] Dyke, S. J., Spencer, B. F., Jr., Sain, M. K., and Carlson, J. D.( 1996). Seismic response reduction using magnetorheological dampers. *Proc., IFAC World Congr.* 145–150.
[5] Dyke, S. J., Spencer, B. F., Jr., Sain, M. K., and Carlson, J. D. (1996).Modeling and control of magnetorheological dampers for seismic response reduction. *Smart Mat. and Struct*. **5**, 565–575.
[6] Yoshida1, O. Dyke, S. (2004).Seismic Control of a Nonlinear Benchmark Building Using Smart Dampers. *Journal of Engineering Mechanics (ASCE),;* **130:4**, 386–392.
[7] Lee H. J., Yang Y. G., Jung H. J.,Spencer B. F., and Lee I. W. (2006).Semi-active neurocontrol of a baseisolated benchmark structure, *Struct. Control Health Monit*. **13**,682–692.
[8] Bani-Hani K. A., and Mashal A. Sheban M. A.(2006). Semi-active neuro-control for base-isolation system using magnetorheological (MR) dampers. *Earthquake Engng Struct. Dyn*. **35**,1119–1144.
[9] Jung H. J., Lee H. J., Yoon W. H., Oh J. W. and Lee I. W. (2004). Semiactive Neurocontrol for Seismic Response Reduction Using Smart Damping Strategy. *Journal of Computing in Civil Engineering*. **18:3**, 277-280.
[10] Choi K-M, Cho S-W, Jung H-J, Lee I-W. (2004).Semi-active f)uzzy control for seismic response reduction using magnetorheological dampers. *Earthquake Engng Struct. Dyn*. **33**,723–736.
[11] Bhardwaj M. K., and Datta T.K.(2006). Semiactive Fuzzy Control of the Seismic Response of Building Frames. *Journal of Structural Engineering,*; **132:5**,791-799.
[12] Kim H-S., and Roschke P. N. (2007). GA-fuzzy control of smart base isolated benchmark building using supervisory control technique. *Advances in Engineering Software*. **38**,453–465.
[13] Mei, G., Kareem, A., and Kantor, J. C. (2001). Real-time model predictive control of structures under earthquakes. *Earthquake Eng. Struct. Dyn*.; **30**,995–1019.
[14] Mei, G., Kareem, A., and Kantor, J. C. (2002).Model predictive control of structures under earthquakes using acceleration feedback. *J. Eng. Mech*,; **128:5**,574–585.
[15] Chang C-C, Zhou L. (2002). Neural network emulation of inverse dynamics for a magnetorheological damper. Journal of Structural Engineering, **128:2**,231–239.
[16] K-karamodin A., H-kazemi H., Rowhanimanesh A.and Akbarzadeh-T M-R. (2007).Semi-active Control of Structures Using Neuro-Inverse Model of MR Dampers. *ISFS2007, First Joint Congress on Intelligent and Fuzzy Systems , Ferdowsi Uni, Mashhad,Iran*.
[17] Ohtori, Y., Christenson, R. E., Spencer, B. F., Jr., and Dyke, S. J. (2004).Benchmark control problems for seismically excited nonlinear buildings. *J. Eng. Mech*.,; **130:4**,366–387.
[18] Dyke, S. J., Yi, F., and Carlson, J. D. (1999). Application of magnetorheological dampers to seismically excited structures. *Proc., Int. Modal Anal. Conf., Bethel, Conn*.
[19] Yi, F., Dyke, S. J., Caicedo, J. M., and Carlson, J. D. (1999). Seismic response control using smart dampers. *Proc. Am. Control Conf., Washington, D.C.* 1022–1026.
[20] Yi, F., Dyke, S. J., Frech, S., and Carlson, J. D. (1998). Investigation of magnetorheological dampers for earthquake hazard mitigation. *Proc., 2nd World Conf. on Struct. Control, West Sussex, U.K*. 349–358.
[21] Spencer, B. F., Jr., Dyke, S. J., Sain, M. K., and Carlson, J. D. (1997). Phenomenological model of magnetorheological damper. *J. Engrg. Mech., ASCE*, **123:3,**230–238.
[22] Hertz J, Krogh A, Palmer RG. (1993). Introduction to the Theory of Neural Computation. Addison-Wesley Publishing Company: Boston, MA,.
[23] The Math Works Inc. (2006). MATLAB 7.0, Natick, MA,.